Dynamics of Water Clusters Confined in Proteins: A Molecular Dynamics Simulation Study of Interfacial Waters in a Dimeric Hemoglobin

Ramachandran Gnanasekaran, Yao Xu, and David M. Leitner*

Department of Chemistry and Chemical Physics Program, University of Nevada, Reno 89557, United States

Received: September 25, 2010; Revised Manuscript Received: November 12, 2010

Water confined in proteins exhibits dynamics distinct from the dynamics of water in the bulk or near the surface of a biomolecule. We examine the water dynamics at the interface of the two globules of the homodimeric hemoglobin from *Scapharca inaequivalvis* (HbI) by molecular dynamics (MD) simulations, with focus on water−protein hydrogen bond lifetimes and rotational anisotropy of the interfacial waters. We find that relaxation of the waters at the interface of both deoxy- and oxy-HbI, which contain a cluster of 17 and 11 interfacial waters, respectively, is well described by stretched exponentials with exponents from 0.1 to 0.6 and relaxation times of tens to thousands of picoseconds. The interfacial water molecules of oxy-HbI exhibit slower rotational relaxation and hydrogen bond rearrangement than those of deoxy-HbI, consistent with an allosteric transition from unliganded to liganded conformers involving the expulsion of several water molecules from the interface. Though the interfacial waters are translationally and rotationally static on the picosecond time scale, they contribute to fast communication between the globules via vibrations. We find that the interfacial waters enhance vibrational energy transport across the interface by ≈10%.

1. Introduction

Water molecules in living cells exhibit dynamics over many time scales depending on environment.[1] Properties of hydration water surrounding biomolecules have been extensively studied both experimentally and computationally in recent years,[2] motivated by the key role water plays in biomolecule structure, dynamics, and function. These studies have detailed the distinction between properties of water in the hydration layer around biomolecules and bulk water.[3−25] Neutron scattering,[26] terahertz (THz) spectroscopy,[11,27,28] and MD simulations[5,9,29] provide information about the typically sluggish dynamics of water at the surface of proteins and dynamical coupling between proteins and water.[11,30,31] The THz absorption coefficient of biological water surrounding saccharides,[32,33] salts,[34] and proteins[35−38] is different from the absorption coefficient of bulk water, allowing measurement of the size of the hydration layer. Water dynamics and spectroscopy depend on a variety of factors, including hydrophobicity of the surface in contact with the water,[39−41] chemical heterogeneity,[42] surface topography,[43−46] and partial confinement. For example, MD simulations on dynamics of water between two domains of the BphC enzyme, with interdomain distances of one to several water layers, reveal how partially confined water molecules between the protein domains translate and rotate significantly slower than water around other regions of the protein. In this article, we explore distinctions between dynamics of clusters of water molecules confined inside proteins and hydration water around them, how this difference is connected to function, and the contribution of confined water to energy flow in the protein. We address the dynamics of 10−20 tightly bound water molecules confined to the interface between the two subunits of the homodimeric hemoglobin (HbI) from the clam *Scapharca inaequivalvis*, which mediate cooperative binding of ligands to the two hemes.[47,48]

Water in nanoconfined environments has generally been observed to relax far more slowly than water in the bulk. Ricci et al.[49] carried out neutron diffraction and deep inelastic neutron scattering experiments on water embedded in silica substrates and found similarities between the confined water and supercooled water in the bulk. Recent MD simulations[50] on water in reverse micelles reveal very slow and curvature-dependent rotational relaxation of water molecules in the reverse micelle, with stretched exponential relaxation and exponents well below 0.5, indicative of glassy dynamics and a wide range of hydrogen-bonding environments. While slow rotational relaxation over tens of picoseconds has been observed in MD simulations for other polar molecules in confined environments,[51] the relaxation of nanoconfined water in reverse miscelles occurs on the nanosecond time scale or longer. We observe a similar size-dependent trend for clusters of water molecules confined in proteins.

We focus in this article on hydrogen bond and rotational dynamics of the interfacial water molecules of HbI. Crystallographic structures of HbI (Figure 1) reveal that the unliganded, deoxy form contains 17 interfacial water molecules, while the liganded, oxy form has 11. In addition to the release of 6 water molecules in going from the deoxy to oxy structure, there are notable tertiary and modest quaternary structural changes, the latter important in the late stages of the allosteric transition.[52,53] Following ligand binding and displacement of the Fe atom, the two heme groups are found further apart.[54,55] Phe97 changes its structural conformation during the transition from the deoxy to oxy state by shifting the phenyl ring to the interfacial hydrated region, so that the volume of the interface is smaller for the oxy form than deoxy-HbI and thus holds less water.[56] Side chains of Asn100 and Lys96 and the propionate group of the hemes form specific hydrogen-bonding arrangements with interfacial waters, arrangements that differ for the liganded and unliganded states. The pivotal role of interfacial water molecules in the allosteric mechanism has been examined by mutation studies.[55,57] Mutations that affect protein−water interactions at the edge of the water cluster in the interface also change the Hill coefficient,[55,58,59] proving that ordered water molecules act as key allosteric mediators in HbI.[60] Molecular dynamics (MD)

* To whom correspondence should be addressed. E-mail: dml@unr.edu.

10.1021/jp109173t © 2010 American Chemical Society
Published on Web 12/02/2010

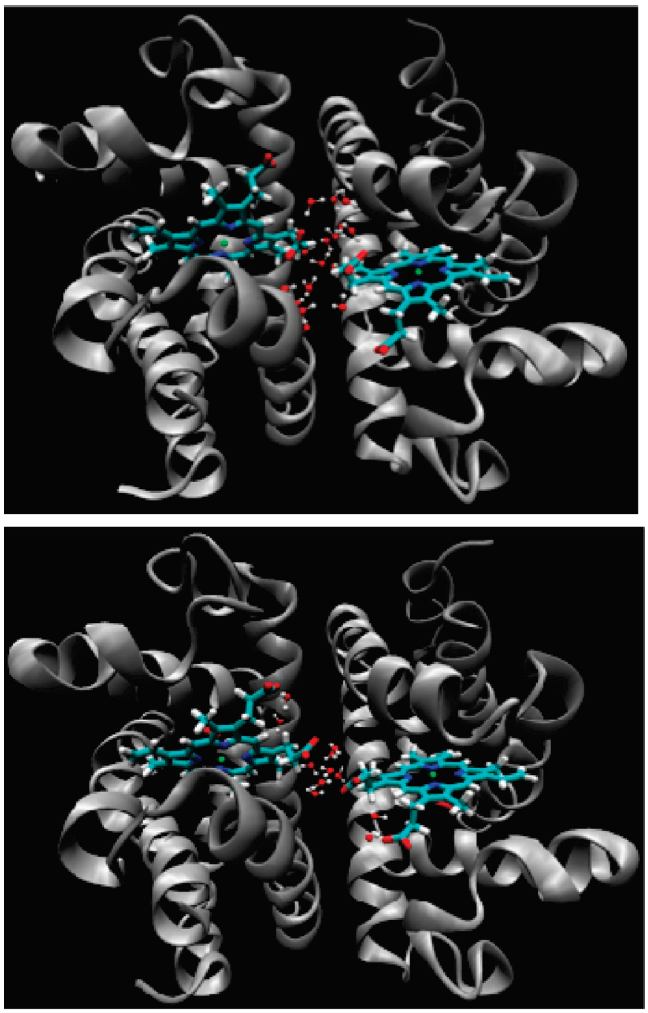

Figure 1. Structures of deoxy- (top) and oxy-homodimeric (bottom) hemoglobin from *Scapharca inaequivalvis* (HbI). The unliganded protein and liganded protein have 17 and 11 water molecules at the interface, respectively.

simulations by Karplus and co-workers[61] elaborated on the role of interfacial water molecules and found that there existed a well-defined water channel that connects the interface between the subunits to bulk water. Although details of the function of the confined waters in HbI cooperativity have not yet been completely worked out, it is clear that the interfacial water is required for efficient communication between the globules.[55]

The MD simulations reported here indicate that rotational relaxation of water molecules at the interface occurs on the 10−1000 ps time scale. Since the interfacial water molecules are embedded inside the protein, they can contribute to fast communication between the globules via vibrational energy transport, which occurs on the 1−10 ps time scale,[23,60,62−67] even if the water is translationally and rotationally static on that short time scale. We consider here the effect of the interfacial water molecules on vibrational energy transport across the interface and find that on the 1−10 ps time scale about 10% more vibrational energy is transferred from a "hot" globule, which has initially excess energy at the heme, over to the "cold", unexcited globule.

The article is organized as follows: In section 2, we detail the computational methods. In section 3A, we present and discuss the results of hydrogen bond time correlation functions, and in section 3B we provide results and discuss rotational reorientation dynamics. In section 3C, we report results of vibrational energy transport across the interface and the influence of the interfacial water molecules on this process. Concluding remarks are provided in section 4.

2. Computational Details

The initial homodimeric hemoglobin structures (oxy-1HbI and deoxy-4SDH) were obtained from the Protein Data Bank (PDB). The first missing residue (proline) was added by using the software package Swiss PDB viewer.[68] We kept the 218 and 219 water molecules included in the crystallographic PDB data for the oxy and deoxy structures, respectively. A cubic box 70 Å on each side was filled with TIP3P water. Following the procedure of Zhou et al.,[61] we kept the 17 and 11 interfacial water molecules of 4SDH and 1HbI, respectively, which are within 10.4 Å of the center of geometry of the deoxy and oxy interface, respectively. The system, now with 12 310 water molecules, was energy-minimized by using the steepest descent algorithm to remove bad contacts. The added solvent water molecules in the simulation box were equilibrated at 300 K for 100 ps by fixing the positions of the protein atoms. The net charge of the system (+4) was neutralized in some of our simulations by addition of counterions, but we found that the addition of counterions to the simulation box did not affect the dynamics of either hydration water or interfacial water on the time scale of our simulations, and the results we report here were obtained without the counterions. The particle-mesh Ewald (PME) method[69,70] was employed to calculate all long-range nonbonded electrostatic interactions by using a 0.12 nm grid and a fourth-order interpolation. The SHAKE algorithm[71] was employed to constrain all bonds to hydrogen and periodic boundary conditions were applied.

All the classical MD simulations and analyses were performed with the GROMACS software package. An NPT ensemble was applied by maintaining the temperature at 300 K with the velocity-rescaling thermostat[72] and by maintaining the pressure at 1 atm with the Parrinello−Rahman barostat.[73] The simulations were performed for 1 ns by integrating the equations of motion with a leapfrog algorithm with integration time steps of 1 fs and the system coordinates were stored every 10 fs. The simulation system consisted of 41 616 (41 612) atoms for oxyhemoglobin (deoxyhemoglobin). We carried out five simulations of 1 ns each for analysis of the hydrogen bond time correlation function and rotational anisotropy. At some point during each of the five 1 ns simulations that we carried out for each system, one water molecule diffused out of the interface and into the hydration layer or the bulk. Once this water molecule escaped, it was no longer considered for analysis of the interfacial water dynamics.

To examine how dynamics of water molecules is affected by the presence of hydration sites at the HbI interface, we have studied the hydrogen bond lifetime correlation function $C_{HB}(t)$, defined as[4]

$$C_{HB}(t) = \frac{\langle h(t)h(0)\rangle}{\langle h\rangle} \tag{1}$$

where h is unity if a hydrogen bond that exists at time 0 still exists at time t and is otherwise 0. We employed standard geometrical criteria for hydrogen bonds; i.e., the distance between donor and acceptor atoms $\leq$0.35 nm and the bond angle between the hydrogen and the acceptor atom is taken as $\leq$30°.

Reorientation of the surface and interfacial water molecules was studied by considering the rotational anisotropy decay, $C_n(t)$, defined as

$$C_n(t) = \langle P_n(\hat{\mu}(t)\cdot\hat{\mu}(0))\rangle \quad (2)$$

where $\hat{\mu}$ is the unit vector pointing along the dipole moment of the water molecule and P_n is the nth degree Legendre polynomial. We specifically considered $n = 1$ and 2, which have been studied in other simulations of hydration water dynamics,[74] as discussed below. For analysis of hydration water molecules, we took all water molecules within the 3 Å layer from the surface of the protein, excluding the interfacial waters.

We also consider vibrational energy flow between the globules. For this analysis, we focus on the deoxy structure and the role of its 17 interfacial water molecules in transferring energy from an initially "hot" globule to a "cold" globule. We specifically simulate excitation of one of the hemes of the protein and follow the transport of kinetic energy, to simulate thermal flow, to other parts of the molecule and water. We in effect heat the heme to 300 K and follow the transfer of energy to the rest of the molecule, which is initially at 0 K, an approach that is analogous to the anisotropic thermal diffusion MD simulations that were carried out on the PDZ domain PSD-95.[75] Since water or solvent molecules generally exchange vibrational energy with peptide units,[76] they may modify energy flow pathways, and we include in our simulations the interfacial water molecules as well as about 1000 hydration water molecules around the protein. We refer to the globule with the heme that is initially 300 K as the hot globule and the other as the cold globule. We carry out the simulation of energy flow in harmonic approximation, since in terms of the normal modes it is both straightforward to propagate the vibrational energy through the system and to give the modes a Boltzmann weight, which effectively freezes out the higher frequency modes from contributing to energy transport, providing a reasonable representation for the population of vibrational modes at a given temperature, as opposed to equipartitioning in a classical simulation. As we see below, the water molecules at the interface do not reorient on the time scale of vibrational energy transport, so the separation of rotational reorientation, translation, and vibrations is very reasonable. We have carried out previous calculations on vibrational energy transport in proteins in this fashion.[77,78]

We carry out propagation and filtering of vibrational wave packets as follows:[79] Consider the kinetic energy, $E_n(t)$, of atom n at time t. We start with a quenched structure and introduce an excitation in the form of a wave packet. The center of kinetic energy, $\mathbf{R}_0(t)$, of the wave packet is found from

$$\mathbf{R}_0(t) = \frac{\sum_n \mathbf{R}_n E_n(t)}{\sum_n E_n(t)} \quad (3)$$

where $\mathbf{R}_n$ is the position of atom n. The variance is

$$\langle \mathbf{R}^2(t)\rangle = \frac{\sum_n (\mathbf{R}_n - \mathbf{R}_0(t))^2 E_n(t)}{\sum_n E_n(t)} \quad (4)$$

We propagate a wave packet expressed as a superposition of the normal modes, starting with an initial wave packet taken to be a traveling wave, where the displacement of atom n initially has the form

$$\mathbf{U}_n(t) = \mathbf{B}_n \exp\left(-\frac{(\mathbf{R}_n - \mathbf{R}' - \mathbf{v}_0 t)^2}{2g^2}\right) e^{i(\mathbf{Q}_0\cdot\mathbf{R}_n - \omega_0 t)} \quad (5)$$

where $\mathbf{R}'$ is the position of the atom at the center of the wave packet, $\mathbf{v}_0$ is the initial velocity, g is the width, $\mathbf{Q}_0$ is the wave vector of the initial excitation, ω_0 is the central frequency of the initial excitation, and $\mathbf{B}_n$ is the amplitude. With this initial wave packet, displacements and velocities at $t = 0$ are determined. Specific values for the variables used in the calculations are given in eqs 8a and 8b. Displacements and velocities for $t > 0$ are then computed in terms of normal modes as

$$\mathbf{U}_n(t) = \sum_\alpha \mathbf{e}_n^\alpha \cos(\omega_\alpha t) \sum_{n'} \mathbf{e}_{n'}^\alpha \cdot \mathbf{U}_{n'}(0) + \sum_\alpha \mathbf{e}_n^\alpha \frac{\sin(\omega_\alpha t)}{\omega_\alpha} \sum_{n'} \mathbf{e}_{n'}^\alpha \cdot \mathbf{V}_{n'}(0) \quad (6a)$$

$$\mathbf{V}_n(t) = \sum_\alpha \mathbf{e}_n^\alpha \cos(\omega_\alpha t) \sum_{n'} \mathbf{e}_{n'}^\alpha \cdot \mathbf{V}_{n'}(0) - \sum_\alpha \mathbf{e}_n^\alpha \omega_\alpha \sin(\omega_\alpha t) \sum_{n'} \mathbf{e}_{n'}^\alpha \cdot \mathbf{U}_{n'}(0) \quad (6b)$$

It is useful to filter the wave packet in frequency around $\bar{\omega} \pm \delta\omega$, for example, with

$$f_\omega = \exp(-(\omega - \bar{\omega})^2/2\delta\omega^2) \quad (7)$$

The positions and velocities are then computed as

$$\mathbf{U}_n(t) = \sum_\alpha \mathbf{e}_n^\alpha \cos(\omega_\alpha t) \sum_{n'} \mathbf{e}_{n'}^\alpha \cdot \mathbf{U}_{n'}(0) f_{\omega_\alpha} + \sum_\alpha \mathbf{e}_n^\alpha \frac{\sin(\omega_\alpha t)}{\omega_\alpha} \sum_{n'} \mathbf{e}_{n'}^\alpha \cdot \mathbf{V}_{n'}(0) f_{\omega_\alpha} \quad (8a)$$

$$\mathbf{V}_n(t) = \sum_\alpha \mathbf{e}_n^\alpha \cos(\omega_\alpha t) \sum_{n'} \mathbf{e}_{n'}^\alpha \cdot \mathbf{V}_{n'}(0) f_{\omega_\alpha} - \sum_\alpha \mathbf{e}_n^\alpha \omega_\alpha \sin(\omega_\alpha t) \sum_{n'} \mathbf{e}_{n'}^\alpha \cdot \mathbf{V}_{n'}(0) f_{\omega_\alpha} \quad (8b)$$

Energy flow from the hot to cold globule was simulated as in previous work on vibrational energy transport in proteins and other polymers[77,79−84] as follows: the initial wave packet expressed as a superposition of the normal modes was centered on the Fe atom. The width of the initial wave packet is $g = 3$ Å. The magnitude of the wave vector of the initial excitation, Q_0, is 0.63 Å^{-1} and it points +45° from the x-, y-, and z-axis; we take $\omega_0 = 9.4$ ps^{-1} and $\mathbf{v}_0 = 20$ Å ps^{-1}, which is reasonably close to the speed of sound in proteins.[65] We checked that our results did not vary significantly with modest changes in these initial conditions. All components of $\mathbf{B}_n$ for all atoms are taken to be the same, and the magnitude is unimportant as it cancels out when we compute the center of energy and its variance. We use a frequency filter whose width, $\delta\omega$, is 50 cm^{-1}, and took the central frequencies to be 10, 50, and 100 cm^{-1}, and continuing in 50 cm^{-1} intervals until 950 cm^{-1}. Thermal results were obtained by taking a thermal average at 300 K over the frequency-resolved results. The temperature of the initially excited region of the protein, in this case the heme, is then 300 K while the rest of the protein is initially at 0 K.

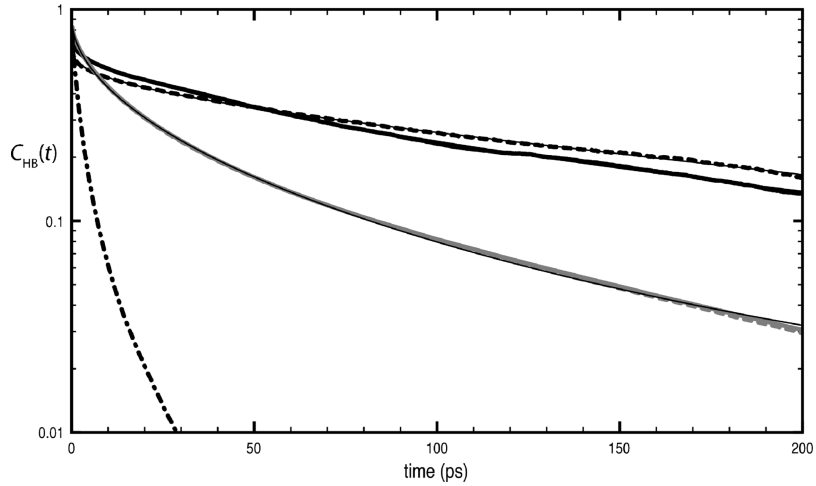

Figure 2. Top two black curves: hydrogen bond time correlation functions, $C_{HB}(t)$, for hydrogen bonds between water and protein for the 11 interfacial water molecules of oxy-HbI (dashed curve) and the 17 water molecules of deoxy-HbI (solid curve). Thin solid lines through $C_{HB}(t)$ are stretched exponentials fit to the computed $C_{HB}(t)$ from 0.2 to 200 ps; the parameters for the fits are listed in Table 1. Gray solid and dashed curves, which are nearly identical, correspond to $C_{HB}(t)$ for hydration waters with the protein for the deoxy and oxy system, respectively. Thin lines through the computed $C_{HB}(t)$ are fits to stretched exponentials. The dot-dashed curve corresponds to $C_{HB}(t)$ computed for hydrogen bonds of pure water.

TABLE 1: Values of β and τ for the Stretched Exponential, $\exp[-(t/\tau)^{\beta}]$, fit to $C_{HB}(t)$ for Hydrogen Bonds between Hydration Water Molecules around Oxy- and Deoxy-HbI and the Protein, and for Hydrogen Bonds between Interfacial Water Molecules and the Protein

	hydration		interfacial	
	β	τ/ps	β	τ/ps
oxy-HbI	0.51	14.2	0.37	39.0
deoxy-HbI	0.52	14.4	0.63	42.0

3. Results and Discussion

3A. Hydrogen Bond Time Correlation Functions. The hydrogen bond correlation functions computed for the hydration and interfacial water molecules are plotted in Figure 2. Relaxation of hydrogen bonds is nonexponential, and we fit the results from 0.2 to 200 ps instead to a stretched exponential, $\exp[-(t/\tau)^{\beta}]$, which, as we see, provides an excellent description of $C_{HB}(t)$ for the results for hydrogen bonds between interfacial waters and the protein and for hydrogen bonds between hydration waters and the protein. The values of τ and β used to fit the results are listed in Table 1. Values of β for the hydration water are essentially the same for the oxy and deoxy structure, 0.51 and 0.52, respectively. The time constants are also similar, 39 and 42 ps, respectively, i.e., both near 40 ps. Unsurprisingly, hydrogen bond lifetimes for water−protein hydrogen bonds at the surface of the proteins do not change in going from the unliganded to the liganded structures, since this transition mainly involves tertiary changes at the interface.

The hydrogen-bonding dynamics of the interfacial waters, however, depends noticeably on ligation. We observe that the hydrogen bonds between interfacial waters and protein, which generally rearrange far slower than the protein−water hydrogen bonds at the surface of the protein, rearrange more slowly for the oxy structure, where we find β to be 0.37, compared with 0.63 for the deoxy structure. While τ is nearly the same for both, 14.2 and 14.4 ps for the oxy and deoxy structures, respectively, it is the much smaller value of β for the interfacial waters of the oxy structure that corresponds to the slow hydrogen bond rearrangement times observed in Figure 2, reflecting a large distribution of hydrogen-bonding environments. The faster rearrangement of the hydrogen bonds between interfacial waters and protein found for the deoxy structure, particularly at longer times, is consistent with the more facile removal of water molecules at the interface, which occurs when ligands bind to the hemes and 6 water molecules are expelled.

Hydrogen bonds between water molecules in the bulk rearrange on a picosecond time scale, as seen in Figure 2, much faster than hydrogen bond rearrangements between water and protein at the interface or in the hydration layer. Hydrogen bond rearrangements in bulk water are nonexponential, but we could not fit the data well to a stretched exponential. The nonexponential decay for bulk water has been observed in a number of previous simulations. Luzar and Chandler[85,86] identified the concerted formation and breaking of hydrogen bonds between water molecules as a possible contributor to nonexponential decay observed in hydrogen bond dynamics. In general, the strengths of hydrogen bonds vary in different environments accounting for differences in kinetic behavior.[87]

A number of earlier computational studies have been carried out to describe water dynamics near the surface of a protein. Concerning hydrogen bond rearrangement and protein−water hydrogen bond lifetimes, Tarek and Tobias[5,88,89] reported MD simulations on hydration water dynamics around ribonuclease A to provide insights into neutron-scattering experiments conducted on hydrated proteins. As part of their analysis they calculated $C_{HB}(t)$ for hydrogen bonds between the protein and water and found it to be nonexponential, relaxing more slowly than hydrogen bond rearrangements between water molecules.[5,89] At about 300 K the former hydrogen bond lifetimes are on the order of 10 ps, but slow dramatically to the nanosecond time scale at temperatures approaching the protein dynamical transition. In related work, water mobility in layers around the protein were examined by Cannistraro and co-workers,[7,90] who carried out MD simulations on solvated plastocyanin and analyzed survival-time-correlation functions for water layers around the protein, finding β from 0.60 to 0.70. Dynamics of hydrogen bonds between water molecules as a function of distance from the surface of a protein in its native conformer and denatured states have been studied by MD simulations.[37,91] Slower hydrogen bond rearrangements near the hydrophobic groups have been observed and attributed[91] to sizable steric hindrance to water mobility near such groups in the systems studied,

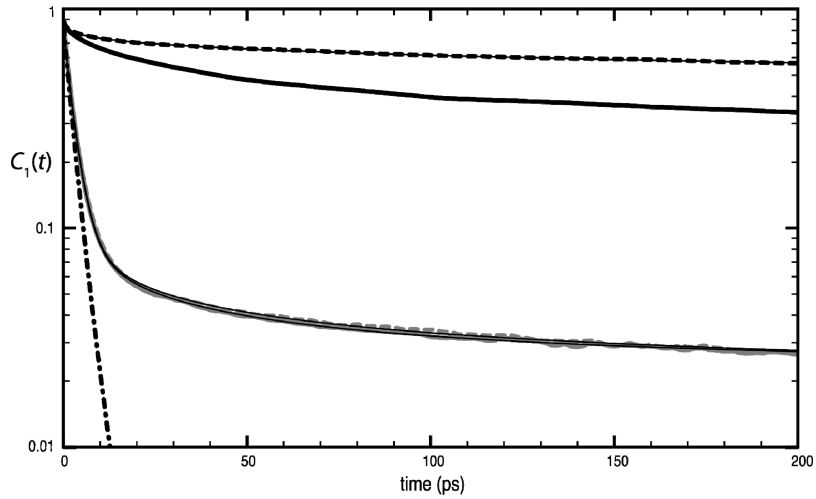

Figure 3. Top two black curves: rotational anisotropy decay functions ($n = 1$), $C_1(t)$, for the 11 interfacial water molecules of oxy-HbI (dashed curve) and the 17 water molecules of deoxy-HbI (solid curve). Thin solid lines through $C_1(t)$ for the interfacial water molecules are stretched exponentials fit to the computed $C_1(t)$ from 0.2 to 200 ps; the parameters for the fits are listed in Table 2. Gray solid and dashed curves, which are nearly identical, correspond to $C_1(t)$ for hydration waters within 3 Å of the protein surface for the deoxy and oxy system, respectively. The dot-dashed curve corresponds to $C_1(t)$ computed for pure water.

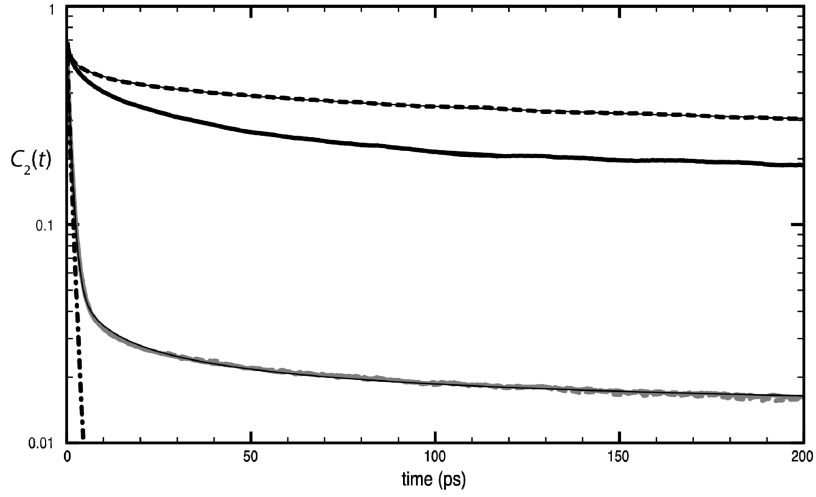

Figure 4. Top two black curves: rotational anisotropy decay functions ($n = 2$), $C_2(t)$, for the 11 interfacial water molecules of oxy-HbI (dashed curve) and the 17 water molecules of deoxy-HbI (solid curve). Thin solid lines through $C_2(t)$ for the interfacial water molecules are stretched exponentials fit to the computed $C_2(t)$ from 0.2 to 200 ps; the parameters for the fits are listed in Table 2. Gray solid and dashed curves, which are nearly identical, correspond to $C_2(t)$ for hydration waters within 3 Å of the protein surface for the deoxy and oxy system, respectively. The dot-dashed curve corresponds to $C_2(t)$ computed for pure water.

consistent with the influence of surface curvature on local water dynamics.[9] For hydrogen bonds between water molecules moving between two protein domains similar trends in the lifetime with distance from the surface of the protein are found, but the lifetimes between the hydrogen bonds are longer than for similar distances around only one domain.[9]

3B. Orientation Dynamics of Surface and Interfacial Water Molecules. Rotational anisotropy decay of order $n = 1$ and 2, defined by eq 2, was computed for the interfacial waters, for all other water molecules within 3 Å of the protein surface, and for bulk water molecules, and the results for C_1 and C_2 are plotted in Figures 3 and 4, respectively. The rotational anisotropy decay for the interfacial water molecules fits well to a stretched exponential, $\exp[-(t/\tau)^{\beta}]$, and the corresponding values of τ and β for fits from 0.2 to 200 ps are listed in Table 2. The anisotropy decay for the hydration water molecules, while nonexponential, fits poorly to a stretched exponential and we note only that the data fit well to the sum of an exponential and stretched exponential, as has been reported in other MD simulation studies of hydration water.[92] A time constant for the hydration water rotational anisotropy decay can be found from the plot if desired. The rotations of the hydration water molecules relax more rapidly than do the rotations of the interfacial waters, and rotations of all waters near the protein relax more slowly than do the rotations of water molecules in the bulk.

TABLE 2: Values of β and τ for the Stretched Exponential, $\exp[-(t/\tau)^{\beta}]$, Fitted to the Rotational Reorientation Correlation Function of Order $n = 1$ and 2 for Interfacial Water Molecules of Oxy- and Deoxy-HbI

		β	τ/ps
oxy-HbI	C_1	0.21	1970.6
	C_2	0.10	70.8
deoxy-HbI	C_1	0.56	140.8
	C_2	0.44	15.6

For both C_1 and C_2, the rotational decay is slower for the interfacial water molecule of oxy-HbI than for deoxy-HbI, the same trend we observed for the hydrogen bond lifetimes discussed above. Considering first C_1, the time constant for the interfacial waters of oxy-HbI is about 2 ns, compared with 141

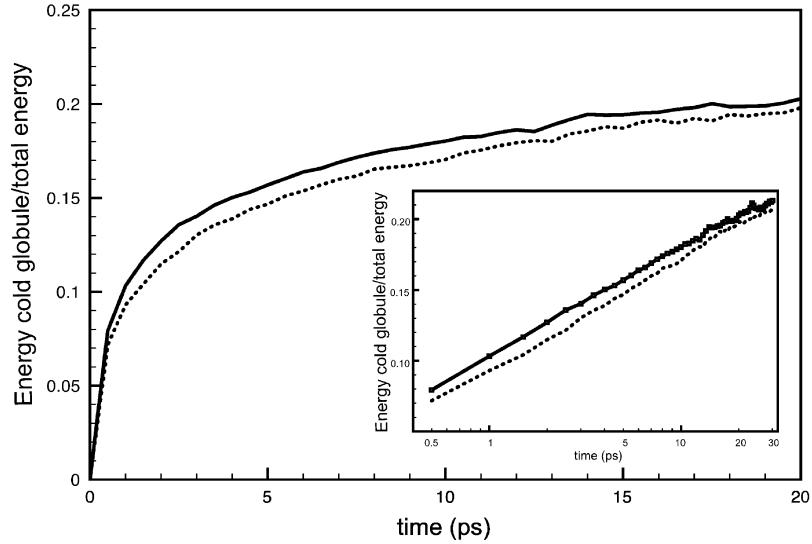

Figure 5. Energy in the initially unexcited, or "cold" globule relative to energy in the entire system is plotted vs time (log(time) in the inset) from 0.5 to 30 ps in 0.5 ps intervals (shown as the points along one of the curves). Dashed curves correspond to this system without the 17 interfacial water molecules. The latter apparently enhance energy transport to the "cold" globule by about 10% for times to about 10 ps.

ps for the interfacial waters of deoxy-HbI. For C_2, these values are 71 and 16 ps, respectively. Values of β are 0.2 and 0.6 for the interfacial waters of oxy- and deoxy-HbI, respectively, for C_1, and they are 0.1 and 0.4, respectively, for C_2. While both C_1 and C_2 have been calculated in previous MD simulations for water in a number of environments, the latter is of additional interest in that it can, with some approximation, be compared with results of polarization-resolved pump−probe experiments.[93] The value for β is especially small for the interfacial waters of oxy-HbI and the time constants particularly large, reflecting the heterogeneity of the hydrogen-bonding environments of the tightly bound water molecules at the interface, particularly for the liganded protein, which has a smaller number of interfacial waters due to its smaller interface volume.

Slow rotational relaxation of water in contact with proteins has been found in many earlier MD simulations. This includes work by Marchi et al.[74] on water around lysozyme. They reported the rotational relaxation of water in the vicinity of lysozyme is 3−7 times slower than that in the bulk, depending on how the hydration shell is defined in the calculation. MD simulations by Oleinikova et al.[92] examined the dynamics of hydration water at the surface of lysozyme at various hydration levels. They reported fits to stretched exponentials for the rotational correlation function at low and high hydration levels. At low hydration level, corresponding to only 200 water molecules at the surface of lysozyme, they found that a stretched exponential equation of the form $\exp[-(t/\tau)^{\beta}]$ with $\beta \approx 0.325$ and relaxation time ≈48 ps fit the data for C_1 well, whereas for higher hydration level C_1 was described by the sum of a stretched exponential and simple exponential. We note also that Cannistraro and co-workers[90] employed simple stretched exponentials to fit the decay of the first- and second-rank rotational reorientation autocorrelation function to 50 ps for water molecules at various distances from the surface of plastocyanin, specifically water molecules in the range 0−4, 0−6, and 0−14 Å. The time constants become smaller as a larger hydration layer is chosen. For the smallest hydration layer, they found time constants of about 10 and 5 ps, respectively, for C_1 and C_2.

Particularly relevant to the calculation of rotational reorientation of water confined in proteins are the MD simulations of Ladanyi, Skinner, and co-workers[50] on water confined in reverse miscelles. They investigated the vibrational spectroscopy and dynamics of water confined inside reverse micelles by calculating correlation functions of spectral densities, hydrogen bonding, and anisotropy decay. They fit the latter to stretched exponentials over times from 0.2 ps to 1 ns, and observed very slow relaxation times and β from 0.17 to 0.37, comparable to values we find for the interfacial waters of HbI, revealing, as in the protein, a highly heterogeneous hydrogen-bonding environment and cooperative, glasslike rearrangements of the confined waters molecules. Rotational reorientation was particularly sluggish for small miscelles, commensurate with the slower relaxation we find when comparing rotational relaxation for the water molecules at the interface of oxy-HbI with those at the interface of deoxy-HbI.

3C. Vibrational Energy Flow Across Interface. We address the contribution of water to energy transport between the globules. The fastest communication between the globules occurs by vibrational energy transport. On the time scale of vibrational energy flow in the protein, which occurs from of order 1 to 10 ps, we have seen the water molecules at the interface to be translationally and rotationally static. We therefore neglect conformational changes due to reorientation of the water molecules while examining vibrational energy flow across the interface, and, as in earlier work,[65,77,82] we consider vibrational energy transport in the harmonic approximation, where it is straightforward to account for the thermal population of the vibrational modes.

We model an experiment where one of the hemes is "heated", as, for example, in recent photolysis experiments that have been carried out on HbI to trigger structural changes that are followed on the nanosecond to microsecond time scale.[94] In the simulation we carry out, we "heat" one of the hemes to 300 K and follow energy transport to the other parts of the protein, which are initially at 0 K, as described in section 2. We focus on the contribution of the interfacial water molecules to vibrational energy transport from the initially hot to the initially cold globule. To do this, we compare results for energy flow from the hot to the cold globule of the protein in its deoxy form with the 17 interfacial water molecules present and when they are absent.

The ratio of the thermal energy calculated for the initially cold globule to the total thermal energy in the system is plotted out to 20 ps in Figure 5 for both the protein with the interfacial waters and the protein excluding these waters. The energy of each globule and of the system is taken as the sum of the kinetic

energy of each atom in that part of the system or in its entirety to reflect relative thermal energies. The results plotted in Figure 5 are averages over the energy ratios we obtained for each of four different structures of the deoxy form, one with and one without interfacial water molecules, from a 100 ps MD simulation, as detailed in section 2. We observe in Figure 5 that, for both proteins, with and without interfacial waters, there is rapid energy flow from the hot to the cold globule in the first 2−3 ps, then slower energy flow in the next ≈10 ps. We also observe enhancement of thermal transport from the hot to the cold globule when the interfacial waters are present. Between 1 and about 10 ps this enhancement is about 10% of the energy transferred. As seen in the inset to Figure 5, we find the ratio of energy in the initially cold globule to energy in the system to vary logarithmically in time over the duration of the simulation, from 0.5 to 30 ps.

4. Concluding Remarks

MD simulations were performed for solvated oxy- and deoxy-HbI systems and the trajectories analyzed to study hydrogen bond and rotational dynamics of water in a cluster that is confined to the interface between the two globules and the water in the hydration layer surrounding the protein. The dynamics of hydration water is retarded by the surface of the protein, as expected, and neither the hydrogen bonds between water and protein nor the rotation of the waters near the protein were affected by protein−ligand binding, which gives rise mainly to rearrangements of side-chain positions at the interface. However, ligand binding strongly affects the much slower dynamics of the 11−17 water molecules clustered at the interface between the two globules of the protein. The interfacial water molecules of the liganded structure of HbI exhibit slower hydrogen bond rearrangement and rotational reorientation than do those of the deoxygenated protein.

The slower relaxation of the interfacial waters found for oxy-HbI compared to the interfacial waters of deoxy-HbI correlates with the smaller volume available at the interface of oxy-HbI, where only 11 water molecules are present, compared to 17 at the interface of deoxy-HbI. The crystal structures indicate that 6 water molecules in each structure form strong hydrogen bonds with charged groups at the interface, including the heme propionate groups. There are 10 hydrogen bonds between interfacial water molecules and side chains in the deoxy structure and 12 in the oxy structure, which probably contributes to the slower dynamics of the waters in the oxy structure. A smaller interface volume means it is more likely that water molecules are in contact with the charged side chains rather than other water molecules. That the water molecules clustered at the interface of the oxygenated structure are more tightly bound than those of the unliganded structure is consistent with the allosteric transition between the two forms, since in the course of the cooperative transition from the deoxy to oxy structures 6 water molecules are expelled from the interface, and these molecules are presumably less tightly bound than the remaining 11. The observation of more tightly bound water in the smaller interface volume of the liganded protein is consistent with results of a recent computational study of dynamics of water confined in reverse miscelles,[50] where slower rotational relaxation and hydrogen bond rearrangements were found to be correlated with a smaller confining volume.

Finally, we examined the contribution of the interfacial waters to vibrational energy transport across the interface between the two globules. On the 1−10 ps time scale of vibrational energy transport through the protein we have seen that the water molecules at the interface, other than vibrating, are essentially static. We find that the interfacial water molecules contribute significantly to fast energy flow across the interface, enhancing vibrational energy transport from one globule to the other by about 10% over the first 10 ps.

Acknowledgment. Support from NSF grant CHE-0910669 is gratefully acknowledged.

References and Notes

(1) Persson, E.; Halle, B. *Proc. Natl. Acad. Sci. U.S.A.* **2008**, *105*, 6266.
(2) Ball, P. *Chem. Rev.* **2008**, *108*, 74.
(3) Pal, S. K.; Peon, J.; Zewail, A. H. *Proc. Natl. Acad. Sci. U.S.A.* **2002**, *99*, 1763.
(4) Bagchi, B. *Chem. Rev.* **2005**, *105*, 3197.
(5) Tobias, D. J. ; Sengupta, N.; Tarek, M. *Proteins: Energy, Heat and Signal Flow*; Leitner, D. M., Straub, J. E., Eds.; Taylor and Francis: New York, 2009.
(6) Stanley, H. E.; Kumar, P.; Han, S.; Mazza, M. G.; Stokely, K.; Buldyrev, S. V.; Franzese, G.; Mallamace, F.; Xu, L. *J. Phys.: Condens. Matter* **2009**, *21*, 504105.
(7) Bizzarri, A. R.; Cannistraro, S. *J. Phys. Chem B* **2002**, *106*, 6617.
(8) Johnson, M. E.; Malardier-Jugroot, C.; Murarka, R. K.; Head-Gordon, T. *J. Phys. Chem. B* **2009**, *113*, 4082.
(9) Hua, L.; Huang, X.; Zhou, R.; Berne, B. J. *J. Phys. Chem. B* **2006**, *110*, 3704.
(10) Wiesner, S. K.; Prendergast, E.; Halle, B. *J. Mol. Biol.* **1999**, *286*, 233.
(11) Leitner, D. M.; Havenith, M.; Gruebele, M. *Int. Rev. Phys. Chem.* **2006**, *25*, 553.
(12) Grebenkov, D. S.; Goddard, Y. A.; Diakova, G.; Korb, J.-P.; Bryant, R. G. *J. Phys. Chem. B* **2009**, *113*, 13347.
(13) Pizzitutti, F.; Marchi, M.; Sterpone, F.; Rossky, P. J. *J. Phys. Chem. B* **2007**, *111*, 7584.
(14) Furse, K. E.; Corcelli, S. A. *J. Phys. Chem. Lett.* **2010**, *1*, 1813.
(15) Furse, K. E.; Corcelli, S. A. *J. Phys. Chem. B* **2010**, *114*, 9934.
(16) Yu, I.; Tasaki, T.; Nakada, K.; Nagaoka, M. *J. Phys. Chem. B* **2010**, *114*, 12392.
(17) Yu, I.; Nagaoka, M. *Chem. Phys. Lett.* **2004**, *388*, 316.
(18) Mitra, L.; Smolin, N.; Ravindra, R.; Royer, C.; Winter, R. *Phys. Chem. Chem. Phys.* **2006**, *8*, 1249.
(19) LeBard, D. N.; Matyushov, D. V. *J. Phys. Chem. B* **2010**, *114*, 9246.
(20) Dadarlat, V. M.; Post, C. B. *Biophys. J.* **2006**, *91*, 4544.
(21) Yu, X.; Park, J.; Leitner, D. M. *J. Phys. Chem. B* **2003**, *107*, 12820.
(22) Chalikian, T. V. *Annu. Rev. Biophys. Biomol. Struct.* **2003**, *32*, 207.
(23) Lervik, A.; Bresme, F.; Kjelstrup, S.; Bedeaux, D.; Rubi, J. M. *Phys. Chem. Chem. Phys.* **2010**, *12*, 1610.
(24) Carey, C.; Cheng, Y.-K.; Rossky, P. *J. Chem. Phys.* **2000**, *258*, 415.
(25) Yu, H.; Rick, S. W. *J. Am. Chem. Soc.* **2009**, *131*, 6608.
(26) Frölich, A.; Gabel, F.; Jasnin, M.; Lehnert, U.; Oesterhelt, D.; Stadler, A.; Tehei, M.; Weik, M.; Wood, K.; Zaccai, G. *Faraday Discuss.* **2009**, *141*, 117.
(27) Knab, J. R.; Chen, J.-Y.; Markelz, A. G. *Biophys. J.* **2006**, *90*, 2576.
(28) Born, B.; Kim, S.-J.; Ebbinghaus, S.; Gruebele, M.; Havenith, M. *Faraday Discuss.* **2009**, *141*, 161.
(29) Makarov, V. A.; Feig, M.; Andrews, B. K.; Pettitt, B. M. *Biophys. J.* **1998**, *75*, 150.
(30) Shenogina, N.; Keblinski, P.; Garde, S. *J. Chem. Phys.* **2008**, *129*, 155105.
(31) Frauenfelder, H.; Fenimore, P. W.; Chen, G.; McMahon, B. H. *Proc. Natl. Acad. Sci. U.S.A.* **2006**, *103*, 15469.
(32) Heugen, U.; Schwaab, G.; Bründermann, E.; Heyden, M.; Yu, X.; Leitner, D. M.; Havenith, M. *Proc. Natl. Acad. Sci. U.S.A.* **2006**, *103*, 12301.
(33) Heyden, M.; Bründermann, E.; Heugen, U.; Niehues, G.; Leitner, D. M.; Havenith, M. *J. Am. Chem. Soc.* **2008**, *130*, 5773.
(34) Schmidt, D. A.; Birer, Ö.; Funkner, S.; Born, B.; Gnanasekaran, R.; Schwaab, G.; Leitner, D. M.; Havenith, M. *J. Am. Chem. Soc.* **2009**, *131*, 18512.
(35) Ebbinghaus, S.; Kim, S.-J.; Heyden, M.; Yu, X.; Heugen, U.; Gruebele, M.; Leitner, D. M.; Havenith, M. *Proc. Natl. Acad. Sci. U.S.A.* **2007**, *104*, 20749.
(36) Kim, S. J.; Born, B.; Havenith, M.; Gruebele, M. *Angew. Chem.* **2008**, *120*, 6486.
(37) Ebbinghaus, S.; Kim, S. J.; Heyden, M.; Yu, X.; Gruebele, M.; Leitner, D. M.; Havenith, M. *J. Am. Chem. Soc.* **2008**, *130*, 2374.
(38) Ebbinghaus, S.; Meister, K.; Born, B.; DeVries, A. L.; Gruebele, M.; Havenith, M. *J. Am. Chem. Soc.* **2010**, *132*, 12210.
(39) Lombardo, T. G.; Giovambattista, N.; Debenedetti, P. G. *Faraday Discuss.* **2009**, *141*, 359.

(40) Dzubiella, J.; Swanson, J. M. J.; McCammon, J. A. *Phys. Rev. Lett.* **2006**, *96*, 087802.
(41) Bresme, F.; Wynveen, A. *J. Chem. Phys.* **2007**, *126*, 044501.
(42) Giovambattista, N.; Debenedetti, P. G.; Rossky, P. J. *J. Phys. Chem. C* **2007**, *111*, 1323.
(43) Hua, L.; Huang, X.; Liu, P.; Zhou, R.; Berne, B. J. *J. Phys. Chem. B* **2007**, *111*, 9069.
(44) Cheng, Y.-K.; Rossky, P. J. *Nature* **1998**, *392*, 696.
(45) Luise, A.; Falconi, M.; Desideri, A. *Proteins: Struct., Funct., Genet.* **2000**, *39*, 56.
(46) Yu, H.; Rick, S. W. *J. Phys. Chem. B* **2010**, *114*, 11552.
(47) Chiancone, E.; Vecchini, P.; Verzilli, D.; Ascoli, F.; Antonini, E. *J. Mol. Biol.* **1981**, *152*, 577.
(48) Royer, W. E.; Love, W. E.; Fenderson, F. F. *Nature* **1985**, *316*, 277.
(49) Ricci, M. A.; Bruni, F.; Giuliani, A. *Faraday Discuss.* **2009**, *141*, 347.
(50) Pieniazek, P. A.; Lin, Y.; Chowdhary, J.; Ladanyi, B. M.; Skinner, J. L. *J. Phys. Chem. B* **2009**, *113*, 15017.
(51) Morales, C. M.; Thompson, W. H. *J. Phys. Chem. A* **2009**, *113*, 1922.
(52) Knapp, J. E.; Pahl, R.; Srajer, V.; Royer, W. E. *Proc. Natl. Acad. Sci. U.S.A.* **2006**, *103*, 7649.
(53) Elber, R. *Biophys. J.* **2007**, *92*, L85.
(54) Knapp, J. E.; Gibson, Q. H.; Cushing, L.; Royer, W. E. *Biochemistry* **2001**, *40*, 14795.
(55) Royer, W. E.; Pardanani, A.; Gibson, Q. H.; Peterson, E. S.; Friedman, J. M. *Proc. Natl. Acad. Sci* **1996**, *93*, 14526.
(56) Royer, W. E.; Hendrickson, W. A.; Chiancone, E. *Science* **1990**, *249*, 518.
(57) Ceci, P.; Giangiacomo, L.; Boffi, A.; Chiancone, E. *J. Mol. Biol.* **2002**, *277*, 6929.
(58) Pardanani, A.; Gambacurta, A.; Ascoil, F.; Royer, W. E. *J. Mol. Biol.* **1998**, *284*, 729.
(59) Pardanani, A.; Gibson, Q. H.; Colotti, G.; Royer, W. E. *J. Biol. Chem.* **1997**, *272*, 13171.
(60) Leitner, D. M.; Straub, J. E. *Proteins: Energy, Heat and Signal Flow*; Taylor and Francis Press: New York, 2009.
(61) Zhou, Y.; Zhou, H.; Karplus, M. *J. Mol. Biol.* **2003**, *326*, 593.
(62) Fujisaki, H.; Straub, J. E. *Proc. Natl. Acad. Sci. U.S.A.* **2005**, *102*, 6726.
(63) Leitner, D. M. *Adv. Chem. Phys.* **2005**, *130B*, 205.
(64) Leitner, D. M. *Annu. Rev. Phys. Chem.* **2008**, *59*, 233.
(65) Yu, X.; Leitner, D. M. *J. Phys. Chem. B* **2003**, *107*, 1698.
(66) Nguyen, P. H.; Park, S. M.; Stock, G. *J. Chem. Phys.* **2010**, *132*, 025102.
(67) Takayanagi, M.; Okumura, H.; Nagaoka, M. *J. Phys. Chem. B* **2007**, *111*, 864.
(68) Guex, N.; Peitsch, M. C. *Electrophoresis* **1997**, *18*, 2714.
(69) Darden, T.; York, D.; Pedersen, L. *J. Chem. Phys.* **1993**, *98*, 10089.
(70) Essmann, U.; Perera, L.; Berkowitz, M. L.; Darden, T.; Lee, H.; Pedersen, L. G. *J. Chem. Phys.* **1995**, *103*, 8577.
(71) Ryckaert, J. P.; Ciccotti, G.; Berendsen, H. J. C. *J. Comput. Phys.* **1997**, *23*, 327.
(72) Bussi, G.; Donadio, D.; Parrinello, M. *J. Chem. Phys.* **2007**, *126*, 014101.
(73) Parrinello, M.; Rahman, A. *J. Appl. Phys.* **1981**, *52*, 7182.
(74) Marchi, M.; Sterpone, F.; Ceccarelli, M. *J. Am. Chem. Soc.* **2002**, *124*, 6787.
(75) Ota, N.; Agard, D. A. *J. Mol. Biol.* **2005**, *351*, 345.
(76) Botan, V.; Backus, E. H. G.; Pfister, R.; Moretto, A.; Crisma, M.; Toniolo, C.; Nguyen, P. H.; Stock, G.; Hamm, P. *Proc. Natl. Acad. Sci. U.S.A.* **2007**, *104*, 12749.
(77) Yu, X.; Leitner, D. M. *J. Chem. Phys.* **2005**, *122*, 054902.
(78) Yu, X.; Leitner, D. M. *J. Chem. Phys.* **2005**, *123*, 104503.
(79) Yu, X.; Leitner, D. M. *Phys. Rev. B* **2006**, *74*, 184305.
(80) Enright, M. B.; Leitner, D. M. *Phys. Rev. E* **2005**, *71*, 011912.
(81) Enright, M. B.; Yu, X.; Leitner, D. M. *Phys. Rev. E* **2006**, *73*, 051905.
(82) Yu, X.; Leitner, D. M. *J. Chem. Phys.* **2003**, *119*, 12673.
(83) Leitner, D. M. *Phys. Rev. B* **2001**, *64*, 094201.
(84) Leitner, D. M. *Phys. Rev. Lett.* **2001**, *87*, 188102.
(85) Luzar, A. *J. Chem. Phys.* **2000**, *113*, 10663.
(86) Luzar, A.; Chandler, D. *Nature* **1996**, *379*, 55.
(87) Xu, H.; Berne, B. J. *J. Phys. Chem. B* **2001**, *105*, 11929.
(88) Tarek, M.; Tobias, D. J. *Biophys. J.* **2000**, *79*, 3244.
(89) Tarek, M.; Tobias, D. J. *Phys. Rev. Lett.* **2002**, *88*, 138101.
(90) Rocchi, C.; Bizzarri, A. R.; Cannistraro, S. *Phys. Rev. E* **1998**, *57*, 3315.
(91) Heyden, M.; Havenith, M. *Methods* **2010**, *52*, 74.
(92) Oleinikova, A.; Smolin, N.; Brovchenko, I. *Biophys. J.* **2007**, *93*, 2986.
(93) Piletic, I. R.; Moilanen, D. E.; Spry, D. B.; Levinger, N. E.; Fayer, M. D. *J. Phys. Chem. A* **2006**, *110*, 4985.
(94) Nienhaus, K.; Knapp, J. E.; Palladino, P.; Royer, W. E.; Nienhaus, G. U. *Biochemistry* **2007**, *46*, 14018.

JP109173T